

## EFFECT OF SURFACTANTS ON DROPLET FORMATION IN MICROCHANNELS

**Ehsan Yakhshi Tafti**  
University of Central Florida  
Orlando, Florida, USA

**Ranganathan Kumar**  
University of Central Florida  
Orlando, Florida, USA

**Kevin Law**  
New College of Florida  
Sarasota, Florida, USA

**Hyoungh J. Cho**  
University of Central Florida  
Orlando, Florida, USA

### ABSTRACT

*It has been well established that droplet based microfluidic systems serve as robust and highly controllable platforms for applications such as micro reactors, chemical and biological assays, drug delivery systems and single cell studies. This paper focuses on the effects of surfactants as a means to control droplet size and generation rate. The frequency of droplet formation at multiple combinations of flow rates of the continuous and dispersed phase is studied as a function of varying surfactant concentrations using a flow focusing and 45° Y junction configurations in microchannels. The microchannels have been fabricated using conventional photolithography and microfabrication techniques. Channels width and depth are 100 micrometers with minimum features size of 25µm at the flow focusing section and the junctions. The results show two distinct regimes of droplet formation for both flow configurations. Increasing surfactant concentration from 0% (pure water) to a critical concentration reduces the generation rate (increased droplet volume); a trend of increasing droplet formation frequency (decreasing droplet size) in both channel systems is observed as surfactant concentration is increased passed the critical value ( 0.01% and 0.05% for Y junction and flow focusing features respectively). Once equilibrium is reached, the droplet formation follows a stable and continuous behavior with variations limited below 10% in rate of generation.*

### INTRODUCTION

Microfluidic droplet generators are valuable tools used in a wide range of applications. Microfluidic droplets have been proposed for use as small-scale chemical reactors [1, 2], where extremely tiny volumes of expensive chemicals must be processed rapidly and efficiently. Microfluidics generated droplets have also been utilized for isolating single living cells for study without killing them [3]. Microfluidic droplets have also been proposed for use as drug delivery systems [4]. Droplets generated with stable frequency and size

have been used both, as substance as well as information carriers, on microfluidic chips containing digital logic gates [5]. An important aspect of studying microfluidic droplet generators is the means of controlling the process of droplet production with high repeatability and stability in terms of size, shape and rate of production. Size, shape, and frequency of droplets are the factors that must be controlled in order to realize any of these applications.

Surface tension causes a droplet to hold its shape. At the boundary between two immiscible liquids, interfacial tension is observed that causes break up of one fluid into the other phase which is known as the carrier or continuous phase. Interfacial tension, shear stress and pressure which result from the flow, geometrical configuration and the physical properties of the fluid and their interplay are known to affect droplet generation. Various theories have been proposed that explain the dynamic interplay between these factors in different flow regimes [6-8]. Flow regimes in binary immiscible phases are categorized using non dimensional numbers as the Reynolds ( $Re = \rho U D_H / \mu$ ) and Capillary ( $Ca = \mu U / \gamma$ ) numbers. ( $\rho$ ,  $U$ ,  $D_H$  and  $\mu$  are fluid density, average flow velocity, critical length scale and fluid viscosity respectively;  $\gamma$  is the interfacial surface tension between working fluids).

There are a variety of methods proposed by various research groups for creating droplets in microchannels. Electrical currents have been used to create microfluidic droplets [9, 10]. Focused acoustic beams have also been applied to fluids to promote droplet formation [11]. However, the most common technique used to form droplets involves junctions and flow focusing features in microchannel using a binary system of water-in-oil or oil-in-water droplets [12]. In a microchannel system, a continuous phase (usually the organic phase) is pumped through a hydrophobic microchannel [13]. The dispersed

phase (aqueous) is pumped through a secondary channel that eventually breaks up into streams of monodispersed droplets. The flow focusing and junction architectures have been used in this experiment as well. The flow focusing device [14] focuses two streams of oil at the secondary channel where the aqueous phase emerges. The two continuous streams, pinch off droplets of water as they flow downstream of the crossflow region. The other channel design is the 45°Y junction. The Y junction consists of a large channel which carries the continuous phase, with a smaller channel directing the dispersed phase at a 90° (or in this case 45°) angle to the main channel. In this study, addition of surfactant that typically reduces surface and interfacial tension, is taken as the independent variable at given flow combinations of the continuous and dispersed phases and droplet size and rate of production are evaluated as the dependent variables.

## DEVICE FABRICATION AND EXPERIMENTAL SETUP

Conventional photolithography was used to create the fluidic devices. SU8 (negative photo resist) was spin-coated on a silicon wafer. The device pattern was transferred from a mask on to the photoresist by UV light exposure. After developing of the photoresist, PDMS and curing agent were poured on top of the features and allowed to cure. The PDMS layer with transferred patterns was bonded to another layer of blank PDMS which closed the channels. Bonding was achieved by plasma treatment of the PDMS surfaces. The hydrophobic PDMS channels [13] used in this experiment are 100  $\mu\text{m}$  wide for the main channel and 25  $\mu\text{m}$  wide for the secondary, dispersed phase channel. All trials used the same flow focusing and Y junction channels.

Flow is generated by a syringe pump that allows desired flowrates into the microdevice. The flowrates of the continuous and dispersed phases were varied in the range of 30-150  $\mu\text{L/hr}$  which corresponds to  $\text{Re}=0.1 - 0.5$  implying a highly laminar flow regime. Oleic acid (oil) is used as the continuous (carrier) phase and deionized water as the aqueous dispersed phase. Based on the physical properties of oil [15] the Capillary number would be in the range of  $\text{Ca}=0.002 - 0.003$ .

It has already been established that variation of flow rate combination of the dispersed and continuous phases can be used to directly control droplet size and generation rate [16]. Higher flow rates of the oil phase equate to higher droplet frequency and as such, smaller droplet volumes for a given flow rate of the dispersed phase. This experiment looks to utilize surfactants as a means to adjust these factors within a given flow rate.

Surfactants, or surface acting agents, are molecules that are composed of a polar head and a nonpolar tail. Since like compounds mix with like solvents, the polar head can interact with the polar water (dispersed phase) while the nonpolar tail can interact with the nonpolar oil (continuous phase.) Surfactants act at the interface of immiscible fluids and change the interfacial tension between the two. Sodium dodecyl sulfate (SDS) is used as surfactant which falls in the *anionic* surfactant category; anionic surfactants (usually sulfate based) have a negatively charged polar head. Concentration of surfactant (based on weight percentage) was varied from no surfactant (0%) to 0.1% in the aqueous phase.

Droplet formation was monitored using an inverted microscope with a CCD recording camera. The low frame rate of the camera (30 frames per second) is a limiting factor in this study because generation rates can easily exceed several hundreds of droplets per second if flow rates are increased. Droplet generation frequency was obtained with image analysis and counting of the number of droplets passing a set boundary in a given amount of time. Also, given the fact that flow rates within each trial are constant, droplet volume can be accurately calculated as well. Figure 1 shows the flow focusing and Y junction microchannels. In the flow focusing configuration, streams of oil enter from the sides and the aqueous phase is introduced from the middle channel. In the Y junction, the carrier fluid flows in the main channel and the aqueous phase enters from the 45° branch. It was observed that T junction features (90° branch) were not as good as the Y branches in terms of stable droplet formation. The channels were flushed with methanol, followed by DI water between each change in surfactant concentration.

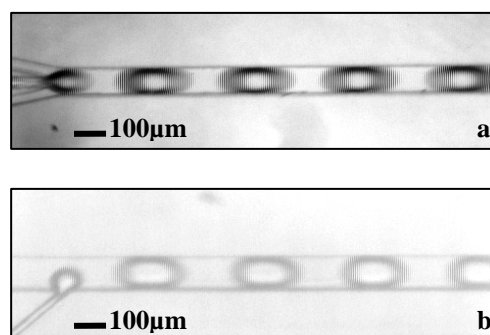


**Figure 1. Flow focusing (a) and 45° Y junction (b) droplet generation features in microchannels**

For each case of flow rate combination of the continuous and dispersed phase, the system was given a minimum of twenty minutes to stabilize before any images were recorded. Tests were performed using four surfactant concentrations: 0% (pure water), 0.01% SDS, 0.05% SDS, and 0.1% SDS. Two higher concentrations were planned (0.5% and 1.0%) but droplet formation was found to become very erratic at concentrations above

0.1% (figure 2). All concentrations listed and used in graphs in this paper are percentages by weight. In molar concentrations, the used values equate to 0.35, 1.75, and 3.50 millimolar solutions.

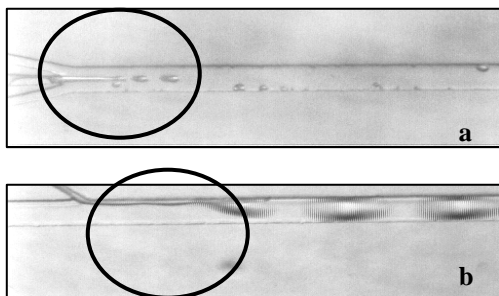


**Figure 2.** Using concentrations above 0.1% produced results such as these. Image (a) shows sporadic, tiny droplets, while image (b) shows no droplet formation, with the two phases moving as side-by-side streams that eventually break up into droplets. The system’s behavior shifted between results such as these over 3-5 minute intervals, with no external changes made to the system

128 frames were recorded for each test case, with the first, last, and middle 64 frames having been analyzed and the results averaged. The variation of droplet generation frequency at given flow cases was seen to be very limited; however there were test cases that the variation reached values up to 10% fluctuation in generation frequency. Droplets were counted as the last visible part in the image disappeared off the edge of the frame.

## RESULTS AND DISCUSSION

Frequency of droplet generation is plotted as a function of surfactant concentration for the Y junction flow configuration in figure 3. All flow configuration show a similar behavior as the surfactant concentration changes. A general trend of increased droplet frequency can be observed as the surfactant concentration increases passing a critical concentration value; below this value droplet rate decreases with addition of surfactant. A similar graph is plotted for the flow focusing device in figure 4. Regarding the fact that the flow rates are kept constant, droplet volume can be calculated by having the rate of droplet generation (number of drops per unit time) the volume of each droplet can be calculated. Typical droplet sizes in this experiment were in the range of 1 – 2 nanoliters.

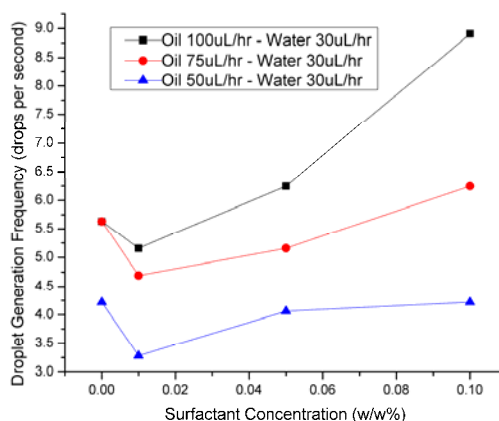


**Figure 3.** Droplet generation rate as a function of surfactant concentration in the aqueous phase for given flow combinations at the Y junction feature

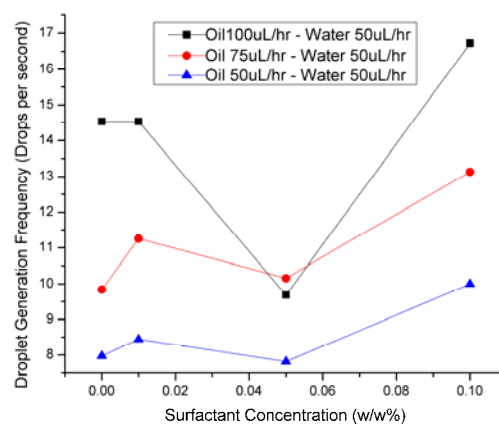


**Figure 4.** Droplet generation rate as a function of surfactant concentration in the aqueous phase for given flow combinations of oil and water at the flow focusing feature

It is expected that with increased surfactant concentrations, the interfacial tension would reduce resulting in easier break up of droplets and eventually higher droplet frequencies. However, in both configurations, this general trend is observed only after passing a critical surfactant concentration (0.01% and 0.05% for Y junction and flow focusing configuration respectively). This finding can be explained as follows. The simplest model for droplet formation is based on the effect of shear forces at the crossflow junction. In this model, the predicted size for a droplet is found by

equating the Laplace pressure with the shear force [17] which gives the spherical droplet size as follows.

$$r \propto \gamma / \mu \dot{\epsilon} \quad (1)$$

$r$  is the droplet radius,  $\gamma$  is the interfacial tension,  $\mu$  is carrier fluid viscosity and  $\dot{\epsilon}$  is the shear rate. According to this theory, it can be said that by increasing the concentration of surfactant, hence reduction of surface tension,  $r$  should steadily decrease if all other parameters stay constant. The graph shows this behavior fairly good for concentration above the value corresponding to the dip in the curves. Another model by Garstecki [18] suggests that at low capillary numbers ( $Ca = \mu U / \gamma$ ), shear forces are not responsible for droplet formation at the junction and the key player is the pressure drop caused by the blockage of the mainstream flow at the junction. According to this theory it can be said that by introducing surfactants, the interfaces of the dispersed phase loosen up, allowing fluid from the side branch to enter the junction and block the mainflow more easily and cause a pressure drop region. Due to the creation of a low pressure region, even more fluid is drawn in from the dispersed phase channel leading to bigger droplets (lower generation frequency). By increasing the percentage of surfactant and further increase in  $Ca$  number (interfacial tension is in the denominator and reduces as concentration of surfactant increases), the process enters a shear regulated regime as mentioned above and viscous (shearing) effects dominate the process and the expected behavior is observed (smaller drops with higher frequency). In summary, two distinct regimes are observed; below the critical concentration, the droplet generation is regulated by pressure forces competing with surface tension and the above the critical value where shear forces and surface effects dominate the process.

It was also observed that for surfactant concentration above 0.1, stable droplets did not form for the higher end of flow rates (Oil 100 $\mu$ L/hr – Water 50 $\mu$ L/hr). Instead the two phases moved side by side as continuous streams, similar to the results found from

using higher concentrations of surfactant. Strangely, when flow rates were lowered, droplets began to form again.

Four data points per graph is a limiting factor in drawing any definitive conclusions from the graphs. Two higher surfactant concentrations were planned to be used; but extreme instability with these concentrations prohibited their use in full testing of such low flow rates. This study was conducted at typically low flow rates due to camera speed limitations. After it was determined that higher concentrations could not be used, several lower intermediate concentrations were tried in order to produce a more well-defined result curve. However, problems began arising with the channels at this point. Flow rates were given up to two hours to stabilize but no stable droplet formation would occur. This means that channel walls had been contaminated permanently once solutions with higher surfactant content were introduced. Although the channels were washed and flushed thoroughly with methanol and DI water prior to testing with the lower surfactant concentration solutions, no stable behavior as previously observed was identifiable. In general, for stable droplet generation, affinity between the continuous phase and the channel wall and the reverse between the dispersed phase and the channel walls are required. In this case oil is the carrier fluid which wets hydrophobic PDMS channel walls unlike the dispersed water phase. It has been shown that the hydrophobicity of PDMS can change over time due to a variety of factors [19]. It is suspected that this change of surface properties may be the primary reason for not being able to reproduce previously recorded data.

## CONCLUSION

45°Y junction and flow focusing features in microchannels were used for droplet generation. The effects of adding surfactants to the aqueous dispersed phase were studied for given flow combinations of the dispersed and continuous phases. In both configurations, there was a dip spotted in the generation rate – concentration curves. This is explained by considering the droplet formation in two distinct regimes; from 0% surfactant up to a critical concentration, the rate of generation decreases (droplet volume increases) while

further addition of surfactant above the critical concentration results in increased droplet generation rate (reduced volume). The first regime is dominated by pressure drop at the crossflows while the latter is affected by the competition of shear (viscous) stress and surface forces.

## REFERENCES

- [1] Klavs, F. J., 1999, "Microchemical Systems: Status, Challenges, and Opportunities," *AICHE Journal*, 45(10), pp. 2051-2054.
- [2] Jensen, K. F., 2001, "Microreaction Engineering -- Is Small Better?," *Chemical Engineering Science*, 56(2), pp. 293-303.
- [3] Demirci, U., and Montesano, G., 2007, "Cell Encapsulating Droplet Vitrification," *Lab Chip*, 7(pp. 1428–1433).
- [4] Shawgo, R. S., Richards Grayson, A. C., Li, Y., and Cima, M. J., 2002, "Biomems for Drug Delivery," *Current Opinion in Solid State and Materials Science*, 6(4), pp. 329-334.
- [5] Toepke, M. W., Abhyankar, V. V., and Beebe, D. J., 2007, "Microfluidic Logic Gates and Timers," *Lab on a Chip*, 7(pp. 1449-1453).
- [6] Tice, J. D., Lyon, A. D., and Ismagilov, R. F., 2004, "Effects of Viscosity on Droplet Formation and Mixing in Microfluidic Channels," *Analytica Chimica Acta*, 507(1), pp. 73-77.
- [7] Tan, Y.-C., Cristini, V., and Lee, A. P., 2006, "Monodispersed Microfluidic Droplet Generation by Shear Focusing Microfluidic Device," *Sensors and Actuators B: Chemical*, 114(1), pp. 350-356.
- [8] Tice, J. D., Song, H., Lyon, A. D., and Ismagilov, R. F., 2003, "Formation of Droplets and Mixing in Multiphase Microfluidics at Low Values of the Reynolds and the Capillary Numbers," *Langmuir*, 19(22), pp. 9127-9133.
- [9] Pollack, M. G., Shenderov, A. D., and Fair, R. B., 2002, "Electrowetting-Based Actuation of Droplets for Integrated Microfluidics," *Lab on a Chip*, 2(pp. 96-101).
- [10] Darren R. Link, E. G.-M. A. D. F. S. Z. C. G. C. M. M. D. A. W., 2006, "Electric Control of Droplets in Microfluidic Devices," *Angewandte Chemie International Edition*, 45(16), pp. 2556-2560.
- [11] Elrod, S. A., Hadimioglu, B., Khuri-Yakub, B. T., Rawson, E. G., Richley, E., Quate, C. F., Mansour, N. N., and Lundgren, T. S., 1989, "Nozzleless Droplet Formation with Focused Acoustic Beams," *Journal of Applied Physics*, 65(9), pp. 3441-3447.
- [12] Nisisako, T., Torii, T., and Higuchi, T., 2002, "Droplet Formation in a Microchannel Network," *Lab Chip*, 2(pp. 24-26).
- [13] Kawakatsu, T., Trägårdh, G., Trägårdh, C., Nakajima, M., Oda, N., and Yonemoto, T., 2001, "The Effect of the Hydrophobicity of Microchannels and Components in Water and Oil Phases on Droplet Formation in Microchannel Water-in-Oil Emulsification," *Colloids and Surfaces A: Physicochemical and Engineering Aspects*, 179(1), pp. 29-37.
- [14] Anna, S. L., Bontoux, N., and Stone, H. A., 2003, "Formation of Dispersions Using 'Flow Focusing' in Microchannels," *Applied Physics Letters*, 82(3), pp. 364-366.
- [15] Gaonkar, A., 1989, "Interfacial Tensions of Vegetable Oil/Water Systems: Effect of Oil Purification," *Journal of the American Oil Chemists' Society*, 66(8), pp. 1090-1092.
- [16] Joanicot, M., and Ajdari, A., 2005, "Applied Physics: Droplet Control for Microfluidics," *Science*, 309(5736), pp. 887-888.
- [17] Thorsen, T., Roberts, R. W., Arnold, F. H., and Quake, S. R., 2001, "Dynamic Pattern Formation in a Vesicle-Generating Microfluidic Device," *Physical Review Letters*, 86(18), pp. 4163.
- [18] Piotr, G., Irina, G., Willow, D., George, M. W., Eugenia, K., and Howard, A. S., 2004, "Formation of Monodisperse Bubbles in a Microfluidic Flow-Focusing Device," *Applied Physics Letters*, 85(13), pp. 2649-2651.
- [19] Meincken, M., Berhane, T. A., and Mallon, P. E., 2005, "Tracking the Hydrophobicity Recovery of Pdm's Compounds Using the Adhesive Force Determined by Afm Force Distance Measurements," *Polymer*, 46(1), pp. 203-208.